Article:
Chen, S. N., Gregori, G., Patel, P. K. et al. (16 more authors) (2007) Creation of hot dense matter in short-pulse laser-plasma interaction with tamped titanium foils. Physics of Plasmas. 102701. -. ISSN: 1089-7674

https://doi.org/10.1063/1.2777118

Creation of hot dense matter in short-pulse laser-plasma interaction with tamped titanium foils

S. N. Chen,[1] G. Gregori,[2,3,a)] P. K. Patel,[4] H.-K. Chung,[4] R. G. Evans,[5] R. R. Freeman,[6] E. Garcia Saiz,[7] S. H. Glenzer,[4] S. B. Hansen,[4] F. Y. Khattak,[7] J. A. King,[1] A. J. Mackinnon,[4] M. M. Notley,[2] J. R. Pasley,[1] D. Riley,[7] R. B. Stephens,[8] R. L. Weber,[6] S. C. Wilks,[4] and F. N. Beg[1]

[1]*University of California, San Diego, La Jolla, California 92093, USA*
[2]*Central Laser Facility, Rutherford Appleton Laboratory, Didcot OX11 OQX, United Kingdom*
[3]*Clarendon Laboratory, University of Oxford, Oxford OX1 3PU, United Kingdom*
[4]*Lawrence Livermore National Laboratory, Livermore, California 94550, USA*
[5]*Department of Physics, Imperial College, London SW7 2AZ, United Kingdom*
[6]*The Ohio State University, Columbus, Ohio 43215, USA*
[7]*School of Mathematics and Physics, Queen's University of Belfast, Belfast BT7 1NN, United Kingdom*
[8]*General Atomics, P.O. Box 85608, San Diego, California 92186, USA*
[9]*Department of Applied Sciences, University of California, Davis, Davis, California 95616, USA*

(Received 21 May 2007; accepted 7 August 2007; published online 2 October 2007)

Dense titanium plasma has been heated to an electron temperature up to 1300 eV with a 100 TW, high intensity short-pulse laser. The experiments were conducted using Ti foils (5 μm thick) sandwiched between layers of either aluminum (1 or 2 μm thick) or plastic (2 μm thick) to prevent the effects of prepulse. Targets of two different sizes, i.e., 250×250 μm^2 and 1×1 mm^2 were used. Spectral measurements of the Ti inner-shell emission, in the region between 4 and 5 keV, were taken from the front-side (i.e., the laser illuminated side) of the target. The data show large shifts in the $K\alpha$ emission from open-shell ions, suggesting bulk heating of the sample at near solid density, which was largest for reduced mass targets. Comparison with collisional radiative and 2D radiation hydrodynamics codes indicates a peak temperature of $T_{e,\mathrm{peak}}=1300$ eV of solid titanium plasma in ~0.2 μm thin layer. Higher bulk temperature ($T_{e,\mathrm{bulk}}=100$ eV) for aluminum tamped compared to CH tamped targets ($T_{e,\mathrm{bulk}}=40$ eV) was observed. A possible explanation for this difference is described whereby scattering due to the nuclear charge of the tamping material leads to modified electron transport behavior. © *2007 American Institute of Physics*. [DOI: 10.1063/1.2777118]

I. INTRODUCTION

Generation of hot dense matter at keV temperatures near solid density in laboratory is necessary for the understanding of radiative and transport processes in inertial confinement fusion (ICF) research[1] and laboratory astrophysics experiments.[2] While the success of ICF requires the solution of a complex interaction between laser coupling, equation-of-state, and particle with radiation transport problems, the possibility of experimentally recreating conditions found in ignition experiments in a simplified and open geometry is important.

There have been extensive studies of ultraintense short-pulse laser absorption physics.[3] However, mechanisms of the heating process in the target, the volume of the heated sample, and magnitude of the temperature gradients have not been thoroughly investigated. Temperatures between 200 and 2000 eV in solid targets have been reported in a variety of experiments.[4–12] Heating of buried Al layers and the effect of a nanosecond pedestal ahead of the main laser pulse have been recently discussed by Evans *et al.*[13] Measurements of density and temperature of hot dense plasmas have been often inferred from spectroscopic techniques, namely intensity ratios[3–12] and wavelength shifts[14] of Lyman and Balmer series lines. Use of only line shapes is not sufficient due to the complexity of atomic radiation transport and absorption within the target, thus it becomes important to infer information using radiation-hydrodynamics, particle-in-cell (PIC), and collisional radiative atomic codes.

Following the initial work of Gregori *et al.*,[4] in this paper we will show that hot dense plasma conditions can be well characterized using a spectral diagnostics technique that is less susceptible to opacity effects. We directly measure the average ionization state of dense titanium plasma by recording the spectral shifts of the $K\alpha$ line emitted from the bulk of the target. Then information about the peak plasma temperatures from the laser heated spot is inferred by measuring the emission from helium-like ions. In addition, we show that the target size and tamper material significantly affect the temperature.

II. EXPERIMENTAL SETUP

The experiment described in this paper was carried out at the Vulcan Laser Facility[15] at the Rutherford Appleton Laboratory (UK). Tamped solid foils were irradiated using the chirped pulse amplified (CPA) arm of the Vulcan laser delivering ~85 J of 1.053 μm p-polarized light with a 1.5 ps pulse length on target. The beam was focused down to

a)Author to whom correspondence should be addressed. Electronic mail: g.gregori@rl.ac.uk

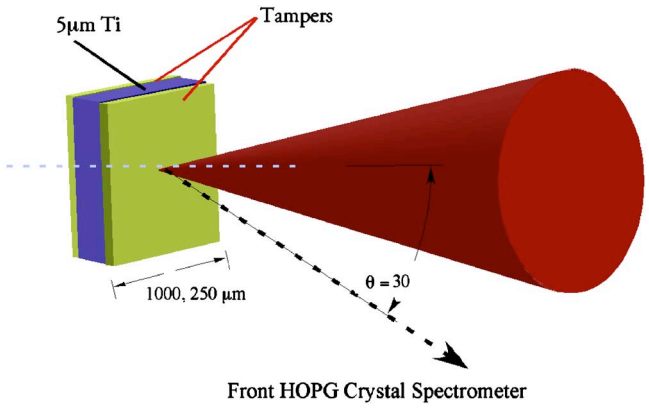

FIG. 1. (Color online) Experimental setup showing the target and the diagnostics viewing angles.

a 10 μm diameter spot by an f/3 off-axis parabola. Focused intensities were on the order of 10^{19} W/cm^2. The targets (see Fig. 1) consisted of a 5 μm thick titanium square either sized 1×1 mm^2 or 250×250 μm^2. The titanium layer was tamped by either 1 or 2 μm Al, or 2 μm CH on the front and the backside of the target by a sputtering technique. The targets were mounted such that their normal was 30° from the laser axis.

A flat highly oriented pyrolytic graphite (HOPG) crystal in 002 orientation[16] coupled to a Fujifilm image plate detector[17] viewed front emission from the target in the 4–5 keV region. The image plate was covered by 5 μm of aluminum to eliminate direct visible light exposure. The spectrometer was protected by a lead housing to reduce background noise from scattered x rays from the chamber wall and diagnostics surrounding the target. The measured spectral resolution of the HOPG crystal was $E/\Delta E=800$ with a dispersion of 0.025 eV/μm.

III. EXPERIMENTAL RESULTS

A. Effect of prepulse

A prepulse (i.e., the presence of a nanosecond pedestal ahead of the main pulse) alters the target conditions by ablating the front surface and produces a long scale length plasma. As shown in Fig. 2, the contrast ratio between the prepulse and the main pulse during the experiment was measured to be $\sim10^7$ and the prepulse duration was $\sim$0.5 ns. Both of these characterizations of the prepulse were performed with a fast diode coupled to an oscilloscope with 20 GS/s sampling rate. In order to minimize the effects of the prepulse, a selection of protective layers, aluminum and CH plastic of various thicknesses, were tested. The Al density (2.7 g/cm^3) is about twice the CH density (1.1 g/cm^3) and we expect a similar ablated mass by the prepulse as indicated by Key[18] at intensities of 10^{13} W/cm^2. The ablation rate for our prepulse level is approximately 10^5 g cm^{-2} s^{-1}. As an input for hydrodynamic simulations, the prepulse was modeled as a 0.5 ns long square pulse with an intensity of 10 TW/cm^2 on a 10 μm spot and 1 ps rise and fall times (see Fig. 2). The 2D radiation-hydrodynamics code h2d (Ref. 19) was used to simulate the effects of this

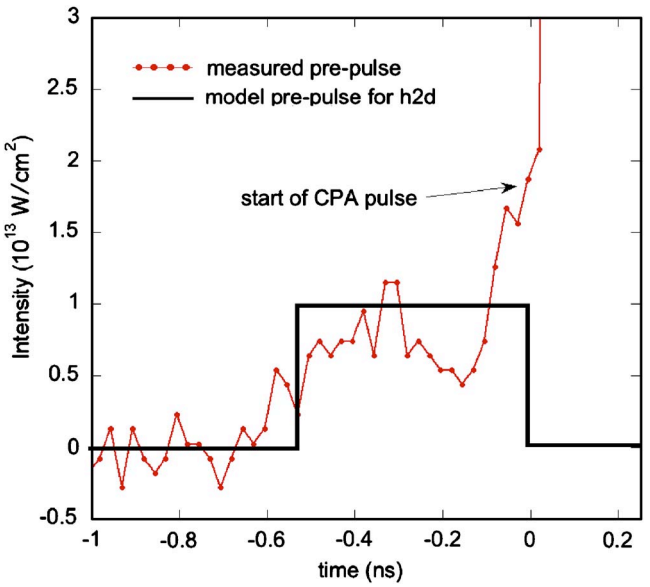

FIG. 2. (Color online) Measured laser prepulse ahead of the main CPA pulse. The solid line corresponds to the modeled pulse in the h2d simulation.

prepulse on the target, as shown in Fig. 3. The h2d package is a two-dimensional (r-z) radiation hydrodynamics code with a multigroup diffusion treatment of radiation transport, flux limited diffusion modeling of electron conduction and Lagrangian hydrodynamics. In these simulations a flux limiter of 0.05 was applied to the electron conduction term, as appropriate for 1ω illumination. The SESAME (Ref. 20) equation of state tables were used, and opacities were generated from an in-line average atom atomic physics model which assumes local thermodynamic equilibrium (LTE). In these simulations 30 radiation groups were employed, arranged logarithmically from 5 eV to 10 keV.

In the simulation results we observe that the 0.5 ns long prepulse launches a shock wave into the target, raising the temperature of the titanium layer to about 1–2 eV, but with the Ti layer remaining at near solid (Fig. 3). In the simulations we have considered both the cases of Al and CH tam-

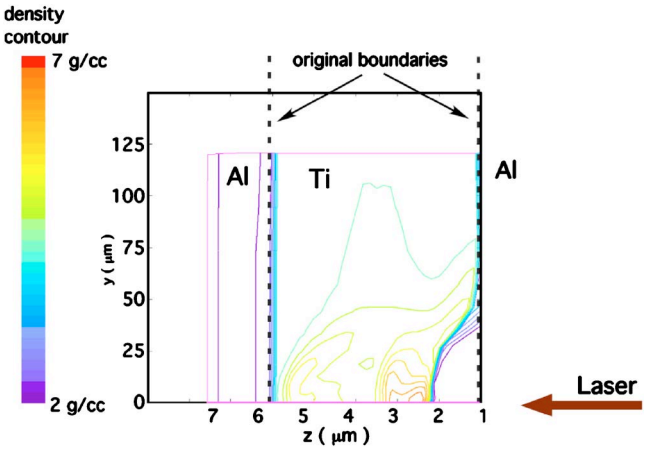

FIG. 3. (Color online) Density contours obtained from h2d simulation of the effect of a 0.5 ns long prepulse on the 250 μm^2 square target tamped with 1 μm Al. The simulation time corresponds to the start of the main laser pulse.

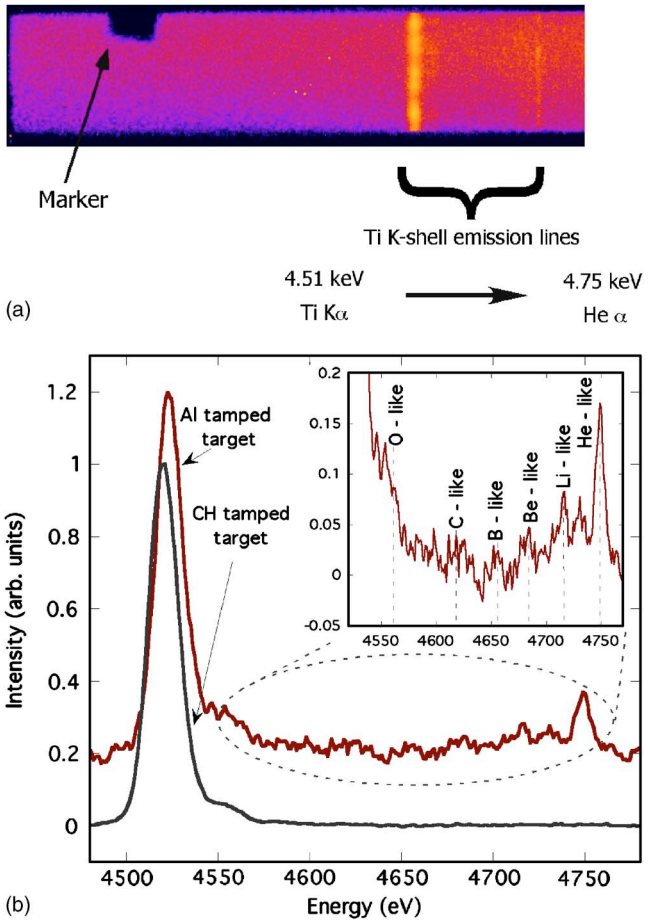

FIG. 4. (Color online) (a) Measured signal on the image plate from the 250×250 μm^2 square target with 1 μm Al tamper. The reference marker is shown on the left and emission lines on the right. (b) Lineout from the exposed image plate of titanium spectra from 4.51 to 4.75 keV of the 1 μm Al tamped target and the 2 μm CH tamped target. Inset shows titanium satellite lines from oxygen-like to helium-like lines.

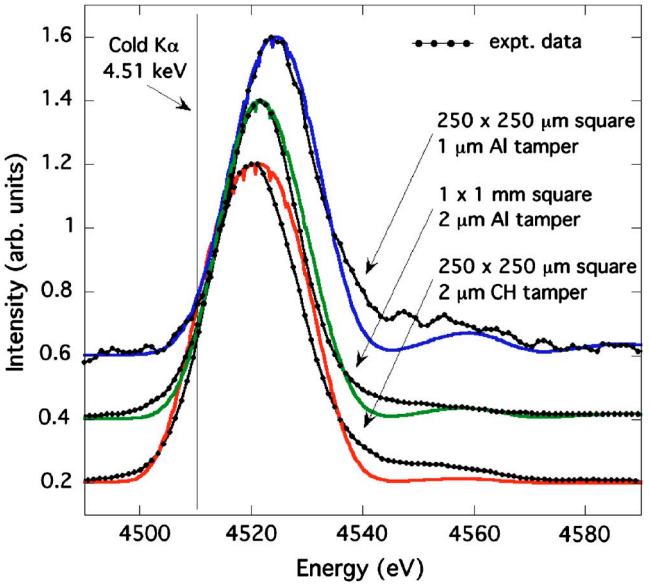

FIG. 5. (Color online) Spectral shifts of cold $K\alpha$ measured by the front spectrometer for various types of targets.

pered foils. The simulation results show that the difference between Al and CH tampers was minimal, likely being a consequence of impedance mismatching effects as the prepulse driven shock wave crosses the interface between the two materials. Along the axis of the laser calculated peak densities were in the order of 7–8 g/cm^3. In each case the tamper acts to keep the Ti layer at or above the original solid density of 4.5 g/cm^3.

B. *K*-shell spectroscopy results

The measured Ti *K*-shell spectrum from a 250×250 μm^2 square target tamped with 1 μm Al is shown in Fig. 4(a). Data were background subtracted and corrected for the 5 μm Al filter transmission. Spectral lineouts, averaged over the nondispersive direction, for both Al and CH tamped cases are shown in Fig. 4(b). The dispersion relating the physical position of the line on the image plate to its corresponding wavelength was calculated by using the Bragg equation, $2d\sin\theta=n\lambda$, where d is the graphite lattice spacing, θ is the Bragg angle, λ is the wavelength, and $n=1$ for first order diffraction. Accounting for the geometry of the spectrometer, a third order analytic dispersion curve was fitted to eight known points given by the theoretical positions of the oxygen-like to the helium-like lines. The absolute position of the $K\alpha$ line is then determined by using the Heα as a reference in conjunction with a marker on the image plate holder [as shown in Fig. 4(a)]. We estimate the absolute error in the energy position of the $K\alpha$ to be ±2.5 eV. The relative error (error between shots) in position between the lines is estimated from the reference marker to be ±1 eV.

In high intensity short pulse laser interactions, with intensities higher than 2×10^{18} W/cm^2, a large number of relativistic electrons ($N_{hot}>10^{14}$) are produced.[21] The electron energies can range from a few keV to tens of MeV. The hot electrons are energetic enough to induce *K*-shell vacancies in titanium with high probability in the solid target. As the sample increases in temperature, the outer electrons of the Ti atom are progressively stripped and thus increasing the *K*-shell ionization potential due to a change in the outer shell shielding. The radiation energy of the $K\alpha$ transition emitted from a partially ionized atom is consequentially shifted with respect to the one which is measured in a neutral system. This change in the x-ray emission has been measured for Ti under the condition of the present experiment, and it is a direct measurement of the ionization state in dense plasmas. Since $K\alpha$ is emitted by the whole target and the measurement is spatially integrated, we can only infer an average (bulk) value representative of the state of the titanium.

Effect of the target size and tamping material

Measurements of the $K\alpha$ line for the three different types of targets (250×250 μm^2 square with 1 μm aluminum tamper, 1×1 mm^2 square with 2 μm aluminum tampers, and 250×250 μm^2 square with 2 μm CH tampers) were used in the experiment and the wavelength of the cold $K\alpha$ line are shown in Fig. 5. We observed smaller shifts in the $K\alpha$ line (~10 eV) with large (1×1 mm^2) targets. The largest shift of ~16 eV was observed with reduced mass targets

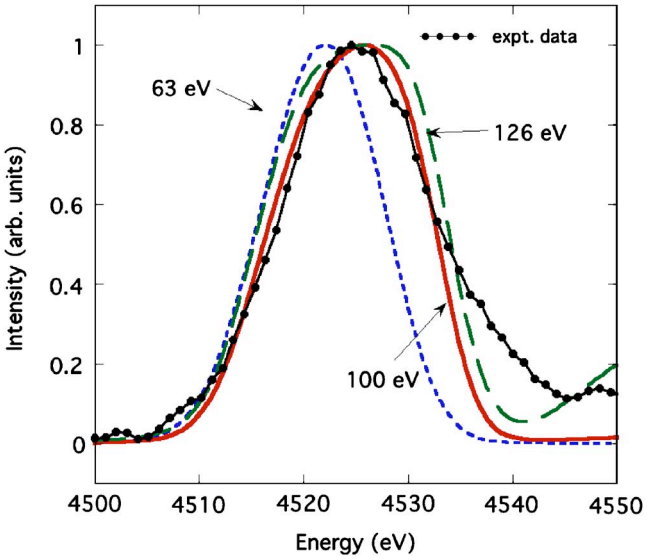

FIG. 6. (Color online) Sensitivity analysis showing the effect of ±2.5 eV error in the absolute energy calibration. The experimental spectrum corresponds to the 250 μm^2 square target with 1 μm Al tamper.

$(250\times250\ \mu m^2)$ and aluminum tampers. However, shifts in the $K\alpha$ position were significantly smaller (<10 eV) when a CH tamper was used in reduced mass targets. The collisional radiative code SCRAM,[22] was used to generate theoretical line shapes for various bulk electron temperatures and to calculate the average ionization state. SCRAM is a collisional radiative model based on hybrid detailed-level and unresolved-transition-array (UTA) data from the FAC code.[23] The model generates rate matrices for a given set of plasma conditions, solves for self-consistent level populations including opacity in the escape factor formalism for a layer of material with fixed thickness, and constructs emission spectra. Two electron populations, one with a bulk thermal temperature of T_e, and a second representing the hot electron temperature T_{hot}=250 keV with a number density of 1% of the total electron population were used. The code is relatively insensitive to the electron distribution function and the average hot electron temperature of the hot electron provided that it is much greater than the ionization energy of the collisional process of interest.

Synthetic spectra generated using the measured instrument response are shown in Fig. 5. The code was run for various thermal temperatures to produce fits with the experimental data. The results from reduced mass targets with a 1 μm Al tamper, which had the largest shift in $K\alpha$ position, indicated bulk temperatures of ~100 eV. With the larger target, the average bulk temperature slightly decreases to 80 eV, which is expected since the mean energy density should decrease with increasing target size.[4] Analysis shows that the error in the absolute wavelength calibration corresponds to an error in the estimated electron temperature of ±20 eV, as indicated in Fig. 6. In reduced mass targets, the number of ions is small, $\sim2\times10^{15}$, and the target is ionized rapidly with a time much smaller than the disassembly time. In contrast to the Al tamped targets, in the case of a CH tamper a significantly lower temperature is observed, of the order of 40 eV.

C. Hot layer temperature

As mentioned before, our measurements show the presence of a significant emission of radiation from highly stripped ions for the case of aluminum tamped targets but not for CH tamped ones [see Fig. 4(b)]. This suggests the presence of a hot ($T_e>800$ eV) region in the aluminum tamped targets. The intensity ratio between the Heα, the intercombination and the lithium-like satellite is very sensitive to temperature, density, and optical thickness of the plasma of interest.[24] We calculated spectra for a range of temperatures, densities, and thicknesses between 0.1 μm and 5 μm with the SCRAM code to extract temperature estimates for the hot plasma region. The best fit for the data from the low-mass target with 1 μm aluminum tamper was obtained with a 0.2 μm thick heated layer of solid titanium at $T_e\sim1300$ eV as shown in Fig. 7(a). Slightly lower hot spot temperatures are obtained with the 1 mm square and 2 μm aluminum tamper. These temperatures are consistent with previous observations of hot layers in short-pulse high-intensity laser plasma interaction with copper planar foils.[25] The temperature error is estimated from Fig. 7(b) to be ±300 eV. Targets tamped with 2 μm CH did not show any evidence of Ti Heα emission, giving an estimated upper limit on T_e of ~500 eV. Thus, both the "hot spot" and bulk temperatures are reduced by at least a factor of two for CH tampers compared with Al tampers of the same mass.

The data described significant temperature differences with the Al and CH tampers. The physics governing transport through this region is extremely complex. There exists several explanations of electron transport through metals and insulators.[26,27] Particularly, Krasheninnikov *et al.*[27] have discussed in detail the growth of electron beam instabilities in insulator targets. One likely explanation for large differences in peak and bulk temperatures arises in the differences in nuclear charge between Al and CH samples. Low current beams of relativistic electrons lose energy due to interaction with bound and free electrons in the solid and also scatter in angle, predominantly due to screened Coulomb collisions with nuclei of charge Z_A. High-current beams behave very differently because their self-generated electric and magnetic fields can dominate the transport and energy loss. These high current beams hugely exceed the Alfvén current and must be largely compensated by a return current in the background thermal plasma. The combination of forward and return currents is unstable to a variety of plasma modes, often loosely referred to as Weibel instabilities.[28] All of these beam instabilities are associated with the beam electrons and have characteristic growth rates on the order of the plasma frequency of the beam species.[29]

The PIC simulations and most of the analytic calculations do not include the effect of angular scattering of the beam electrons by the background plasma. At solid densities this scattering rate can be appreciable and increases strongly with nuclear charge Z_A. Davies *et al.*[30] in their consideration

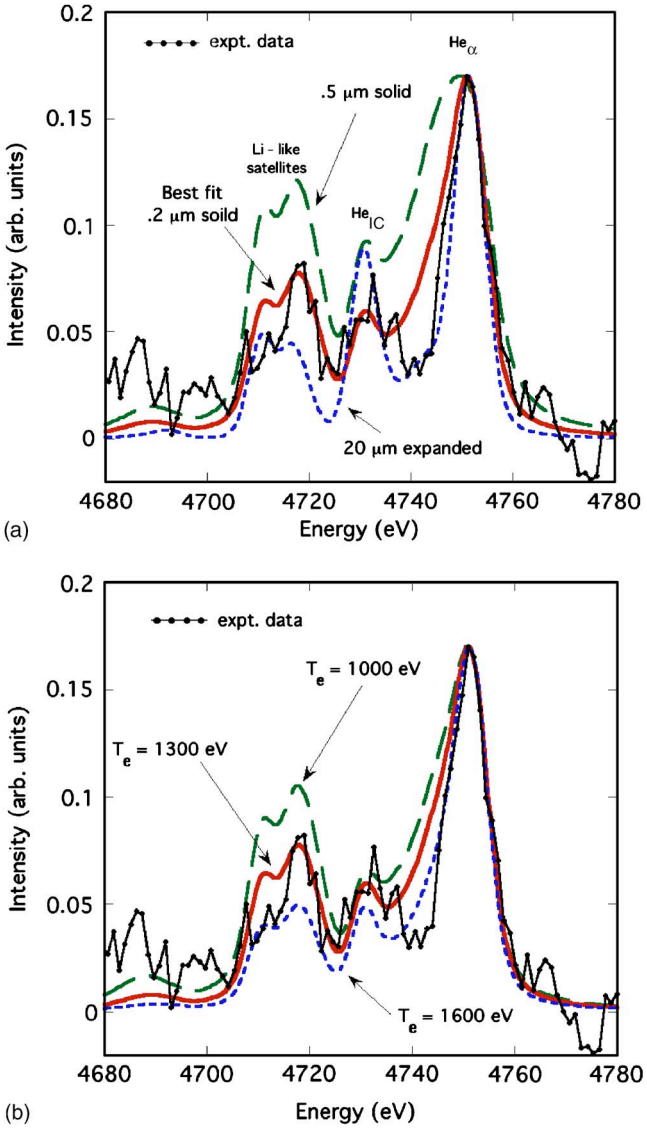

FIG. 7. (Color online) (a) The experimental spectrum for the 250 $\times 250$ μm^2 square target with 1 μm Al tamper is compared with SCRAM calculations: (solid red line) best fit assuming Ti at solid density, T_e =1.3 keV in 0.2 μm hot layer; (dotted blue line) simulation assuming the 0.2 μm layer expanded to a density 100 times lower than solid; (dashed green line) simulation assuming a layer thickness of 0.5 μm. The calculated spectra have been convolved with the experimental instrument response. (b) Sensitivity analysis showing the differences in line intensity of 0.2 μm thick, solid-density Ti at three different temperatures.

of the transport of high current relativistic electron beams show that an electron beam initially with no transverse velocity will acquire a transverse temperature. In particular, they have shown that the average mean square angular scatter can be expressed as

$$\langle \Delta\theta^2 \rangle = \left(\frac{Z_A^2 n e^4}{2\pi\varepsilon_0^2} \frac{\gamma m}{p^3} \ln\Lambda \right) t = \nu_\perp t, \tag{1}$$

where n and m are the number density and mass of the electrons in the background plasma, respectively. The Lorentz factor is γ and p is the relativistic momentum. The Coulomb logarithm is $\ln\Lambda$. Equation (1) is valid for $\Delta\theta \ll 1$ and it shows that an electron beam initially with no transverse velocity spread will acquire a transverse temperature, that in moderate Z_A plasmas increase approximately linearly with time since the angular scattering is faster than the slowing down of the beam. If the initial electron beam is relativistic and $\beta_\perp$ is the transverse velocity normalized to the speed of light, then

$$\beta_\perp^2 = \langle \Delta\theta^2 \rangle.$$

Silva *et al.*[31] have shown that transverse filamentation instability is stabilized by a relatively small transverse temperature in the electron beam. They calculated that for a beam with a longitudinal velocity $\beta_{II}c$, the threshold for filamentation instability is

$$\alpha > \gamma \frac{\beta_\perp^2}{\beta_{II}^2},$$

where α is the ratio of the density of the beam electrons to the density of the background electrons. As discussed previously, for the laser irradiance considered here, $\alpha \sim 10^{-2}$ (see also Evans[32]).

The importance of the angular scattering is that in moderate Z_A materials it is large enough that within one growth time for the filamentation instability the electron beam can acquire through collisions a transverse temperature that is large enough to stabilize the filamentation. The parameter describing the competition between the two effects is $\gamma_f/\nu_\perp$, where γ_f the instability growth rate is of order ω_{pb} the plasma frequency for the beam electrons. This is the number of instability growth times before the transverse velocity spread is large enough to stabilize the instability. Taking a beam of 1 MeV electrons we then find $\gamma_f/\nu_\perp = 14$ for CH and $\gamma_f/\nu_\perp = 0.5$ for Al. Thus, in CH tamped targets the filamentation instability can grow as seen in the PIC simulations,[30] whereas in Al and higher Z_A tamped targets the growth in transverse beam temperature due to scattering stabilizes the filamentation and the stopping is only dependent on the classical collisions and the electric field.

IV. SUMMARY

We have explored a platform for the generation of hot dense matter in the laboratory using short pulse lasers. We have found that, using low mass targets with thin 1 μm aluminum tampers, 100 eV average bulk temperature, and peak temperature of 1300 eV at solid density can be reached. Average ionization state of the solid titanium layer is directly measured by shifts of $K\alpha$ radiation, and bulk temperature inferred from a collisional radiative code. The measurements also indicate significant emission of radiation from highly stripped ions at solid density, suggesting the presence of a hot region, which implies anomalous stopping in the surface layer. Lower bulk temperatures seen with the CH tamped target indicates inhibition of electron transport and we speculate that this may be attributed to increase filamentation in the CH tamper due a lower Z when compared to an aluminum tamper. Clear differences in bulk temperature between plastic and aluminum coated foils have been observed. It is

speculated that this may be attributed to the formation of a transverse temperature in the hot electron beam which stabilizes filamentation.

ACKNOWLEDGMENTS

The authors would like to thank M. Tolley, C. Spindloe, and the target fabrication group at the Central Laser Facility for their constant support during the experiment. Useful discussions with Dr. K. Akli at the Lawrence Livermore National Laboratory and Dr. M-S. Wei of UCSD are kindly acknowledged.

This work was supported by the Science and Technology Facilities Council of the United Kingdom, and partially under the auspices of the U.S. Department of Energy by the University of California Lawrence Livermore National Laboratory under Contract No. W-7405-Eng-48. S.N.C. was supported by the Campus Laboratory Collaboration Program administered by the President of the University of California (USA) and by the Fusion Science Center under the U.S. Department of Energy Grant No. DE-FC03-92SF19460. The h2d simulations were performed with the corporate support of General Atomics.

[1] J. D. Lindl, *Inertial Confinement Fusion* (Springer-Verlag, New York, 1998).
[2] B. A. Remington, R. P. Drake, and D. D. Ryutov, Rev. Mod. Phys. **78**, 755 (2006).
[3] R. R. Freeman, D. Batani, S. Baton, M. Key, and R. Stephens, Fusion Sci. Technol. **49**, 297 (2006), and references therein.
[4] G. Gregori, S. B. Hansen, R. Clarke *et al.*, Contrib. Plasma Phys. **45**, 284 (2005).
[5] A. Saemann, K. Eidmann, I. E. Golovkin, R. C. Mancini, E. Andersson, E. Forster, and K. Witte, Phys. Rev. Lett. **82**, 4843 (1999).
[6] C. Y. Chien, J. S. Coe, G. Mourou, J. C. Kieffer, M. Chaker, Y. Beaudoin, O. Peyrusse, and D. Gilles, Opt. Lett. **18**, 1535 (1993).
[7] Z. Jiang, J. C. Kieffer, J. P. Matte, M. Chaker, O. Peyrusse, D. Gilles, G. Korn, A. Maksimchuk, S. Coe, and G. Mourou, Phys. Plasmas **2**, 1702 (1995).
[8] K. B. Wharton, S. P. Hatchett, S. C. Wilks, M. H. Key, J. D. Moody, V. Yanovsky, A. A. Offenberger, B. A. Hammel, M. D. Perry, and C. Joshi, Phys. Rev. Lett. **81**, 822 (1998).
[9] E. Martinolli, D. Batani, E. Perelli-Cippo *et al.*, Laser Part. Beams **20**, 171 (2002).
[10] K. Eidmann, U. Andiel, F. Pisani, P. Hakel, R. C. Mancini, G. C. Junkel-Vives, J. Abdallah, and K. Witte, J. Quant. Spectrosc. Radiat. Transf. **81**, 133 (2003).
[11] H. Nishimura, T. Kawamura, R. Matsui *et al.*, J. Quant. Spectrosc. Radiat. Transf. **81**, 327 (2003).
[12] J. A. Koch, Y. Aglitskiy, C. Brown *et al.*, Rev. Sci. Instrum. **74**, 2130 (2003).
[13] R. G. Evans, E. L. Clark, R. T. Eagleton *et al.*, Appl. Phys. Lett. **86**, 191505 (2005).
[14] A. Sengebusch, S. H.Glenzer, A. L. Kritcher, H. Reinholz, and G. Roepke, Contrib. Plasma Phys. **47**, 309 (2007); A. L. Kritcher, P. Neumayer, M. K. Urry, H. Robey, C. Niemann, O. L. Landen, E. Morse, and S. H. Glenzer, High Energy Density Physics **3**, 156 (2007).
[15] C. N. Danson, J. Collier, D. Neely *et al.*, J. Mod. Opt. **45**, 1653 (1998).
[16] A. Pak, G. Gregori, J. Knight, K. Campbell, D. Price, B. Hammel, O. L. Landen, and S. H. Glanzer, Rev. Sci. Instrum. **75**, 374 (2004).
[17] J. Miyahara, K. Takahashi, Y. Amemiya, N. Kamiya, and Y. Satow, Nucl. Instrum. Methods Phys. Res. A **246**, 572 (1986).
[18] M. H. Key, W. T. Toner, T. J. Goldsack, J. D. Kilkenny, S. A. Veats, P. F. Cunningham, and C. L. S. Lewis, Phys. Fluids **26**, 7 (1983).
[19] h2d is a commercial product of Cascade Applied Sciences Incorporated, 6325 Trevarton Drive, Longmont, CO 80503 (electronic mail: larsen@casinc.com).
[20] See National Technical Information Service Document No. DE94011699, "SESAME database" by J. D. Johnson, Los Alamos National Laboratory Report No. LA-UR-94–1451, 1994. Copies may be ordered from the National Technical Information Service, Springfield, VA 22161.
[21] F. N. Beg, M. S. Wei, E. L. Clarke *et al.*, Phys. Plasmas **11**, 2806 (2004).
[22] S. B. Hansen, Ph.D. thesis, University of Nevada, Reno (2003); S. B. Hansen, J. Bauche, C. Bauche-Arnoult, and M. F. Gu, High Energy Density Physics **3**, 109 (2007).
[23] M. F. Gu, Astrophys. J. **590**, 1131 (2003).
[24] S. H. Glenzer, C. A. Back, K. G. Estabrook, B. J. MacGowan, D. S. Montgomery, R. K. Kirkwood, J. D. Moody, D. H. Munro, and G. F. Stone, Phys. Rev. E **55**, 927 (1997).
[25] W. Theobald, K. Akli, R. Clarke *et al.*, Phys. Plasmas **13**, 043102 (2006); K. U. Akli, M. H. Key, H. K. Chung. *et al.*, *ibid.* **14**, 023102 (2007).
[26] J. Fuchs, T. E. Cowan, P. Audebert, H. Ruhl *et al.*, Phys. Rev. Lett. **91**, 255002 (2003), and references therein.
[27] S. I. Krasheninnikov, A. V. Kim, B. K. Frolov, and R. Stephens, Phys. Plasmas **12**, 073105 (2005), and references therein.
[28] E. S. Weibel, Phys. Rev. Lett. **2**, 83 (1959).
[29] M. Honda, J. Meyer-ter-Vehn, and A. Pukov, Phys. Plasmas **7**, 1302 (2000).
[30] J. R. Davies, A. R. Bell, M. G. Haines, and S. M. Guerin, Phys. Rev. E **56**, 7193 (1997).
[31] L. O. Silva, R. A. Fonseca, J. W. Tonge, W. B. Mori, and J. M. Dawson, Phys. Plasmas **9**, 2458 (2002).
[32] R. G. Evans, High Energy Density Physics **2**, 35 (2006).